

DOI:10.1002/ejic.201300889

# Nanoscaled Bismuth Oxido Clusters: Probing Factors of Structure Formation and Photocatalytic Activity

Maik Schlesinger,<sup>[a]</sup> Marcus Weber,<sup>[a]</sup> Tobias Rüffer,<sup>[b]</sup>  
Heinrich Lang,<sup>[b]</sup> and Michael Mehring\*<sup>[a]</sup>

*Dedicated to Professor Werner Uhl on the occasion of his 60th birthday*

**Keywords:** Bismuth / Nanostructures / Cluster compounds / Hydrolysis / Photocatalysis

Hydrolysis of bismuth(III) nitrate in the presence of sodium benzoate (NaOBz) in dimethyl sulfoxide (DMSO) gave the bismuth oxido cluster  $[(\text{Bi}_{38}\text{O}_{45}(\text{NO}_3)_{20}(\text{OBz})_4(\text{DMSO})_{24}) \cdot 4\text{DMSO}][(\text{Bi}_{38}\text{O}_{45}(\text{NO}_3)_{24}(\text{DMSO})_{26}) \cdot 4\text{DMSO}]$  (**1**), which crystallizes in the monoclinic space group  $P2_1/c$  with cell parameters of  $a = 35.8728(12)$  Å,  $b = 20.2750(5)$  Å,  $c = 34.8624(11)$  Å, and  $\beta = 111.797(4)^\circ$ . The asymmetric unit contains two crystallographically independent bismuth oxido clusters of different composition. Because of the distinct structural relationship of this type of bismuth oxido clusters with the photocatalytically active polymorph  $\beta$ - $\text{Bi}_2\text{O}_3$ , colloidal

suspensions of nanoscaled **1** as well as colloids composed of the recently reported clusters  $[\text{Bi}_6\text{O}_4(\text{OH})_4(\text{NO}_3)_6] \cdot \text{H}_2\text{O}$  (**2**),  $[(\text{Bi}_{38}\text{O}_{45}(\text{NO}_3)_{24}(\text{DMSO})_{26}) \cdot 2\text{DMSO}][(\text{Bi}_{38}\text{O}_{45}(\text{NO}_3)_{24}(\text{DMSO})_{24}) \cdot 0.5\text{DMSO}]$  (**3**), and  $[\text{Bi}_{38}\text{O}_{45}(\text{OMc})_{24}(\text{DMSO})_9] \cdot 2\text{DMSO} \cdot 7\text{H}_2\text{O}$  (**4**) were probed for their photocatalytic activity. The bismuth oxido cluster **3** decomposes more than 85 % of a  $1 \times 10^{-5}$  M aqueous solution of rhodamine B (RhB) under visible-light irradiation within 150 min. Colloids of such clusters might serve as model compounds for indirect photodegradation processes of organic contaminants at the metal oxide surface.

## Introduction

It is well known that bismuth(III) nitrate tends to hydrolyze quickly and forms various condensation products (at low pH values), so-called bismuth subnitrates. The phenomenon has been known since the Middle Ages, when “bismutum subnitricum” was administered for the treatment of dyspepsia. Remarkably, such formulations are still in use for wound-healing agents.<sup>[1]</sup> However, the composition of bismuth subnitrate as obtained from aqueous solution is ill defined and is often described as a mixture of  $\text{BiONO}_3$ ,  $\text{Bi}(\text{NO}_3)(\text{OH})_2$ , and  $\text{BiOOH}$ .<sup>[2]</sup> Recently it was shown that, when starting from acidic aqueous solutions of bismuth(III) nitrate, the formation of hexanuclear bismuth oxido clusters of the type  $[\text{Bi}_6\text{O}_{4+x}(\text{OH})_{4-x}]^{(6-x)+}$  ( $x = 0, 1$ ) is favored.<sup>[3]</sup> These complex ions result from intramolecular condensation of hydrated  $\text{Bi}^{3+}$  ions<sup>[4]</sup> and represent the largest bismuth oxido clusters that have been crystallized from aqueous media so far.<sup>[5]</sup> However, the use of polar

solvents such as dimethyl sulfoxide (DMSO), acetone, and  $\text{CH}_2\text{Cl}_2$  gave access to several ligand-stabilized  $[\text{Bi}_{38}\text{O}_{44+x}]^{(26-x)+}$  ( $x = 0, 1$ ) clusters.<sup>[5,6]</sup> Such bismuth oxido clusters are composed of 13  $[\text{Bi}_6\text{O}_{8+x}]^{2(1-x)+}$  units ( $x = 0, 1$ ) and represent an additional intermediate within the nucleation process of bismuth oxido/hydroxido nitrates to finally result in  $\text{Bi}_2\text{O}_3$ . It is worth noting that the hexanuclear motifs are present as structural units in the solid-state structures of  $\beta$ - and  $\delta$ - $\text{Bi}_2\text{O}_3$ .<sup>[6a,7]</sup> Thus, the bismuth oxido clusters are excellent precursors for the synthesis of  $\beta$ - $\text{Bi}_2\text{O}_3$  nanoparticles, which show high photocatalytic activity under visible-light irradiation as reported earlier.<sup>[8]</sup> However, metal oxido clusters themselves are also well known for their photocatalytic activity,<sup>[9]</sup> and recently the efficient photodegradation of dyes by using the heterobimetallic bismuth-containing cluster  $\text{H}_3\{[\text{Bi}(\text{DMSO})_3]_4\text{V}_{13}\text{O}_{40}\}$  was reported.<sup>[10]</sup> This prompted us to study the photocatalytic performance of homometallic bismuth oxido clusters, which has not been reported so far. Thus, colloidal suspensions of the following nanoscaled clusters were tested:  $[(\text{Bi}_{38}\text{O}_{45}(\text{NO}_3)_{20}(\text{OBz})_4(\text{DMSO})_{24}) \cdot 4\text{DMSO}][(\text{Bi}_{38}\text{O}_{45}(\text{NO}_3)_{24}(\text{DMSO})_{26}) \cdot 4\text{DMSO}]$  (**1**),  $[\text{Bi}_6\text{O}_4(\text{OH})_4(\text{NO}_3)_6] \cdot \text{H}_2\text{O}$  (**2**),<sup>[3a]</sup>  $[(\text{Bi}_{38}\text{O}_{45}(\text{NO}_3)_{24}(\text{DMSO})_{26}) \cdot 2\text{DMSO}][(\text{Bi}_{38}\text{O}_{45}(\text{NO}_3)_{24}(\text{DMSO})_{24}) \cdot 0.5\text{DMSO}]$ <sup>[5]</sup> (**3**), and  $[\text{Bi}_{38}\text{O}_{45}(\text{OMc})_{24}(\text{DMSO})_9] \cdot 2\text{DMSO} \cdot 7\text{H}_2\text{O}$ <sup>[6b]</sup> (**4**). The photodegradation of rhodamine B (RhB) using visible-light irradiation under the same conditions as reported for  $\beta$ -

[a] Technische Universität Chemnitz, Fakultät für Naturwissenschaften, Institut für Chemie, Professur Koordinationschemie, 09107 Chemnitz, Germany  
E-mail: michael.mehring@chemie.tu-chemnitz.de  
<http://www.tu-chemnitz.de/chemie/koord/index.php>

[b] Technische Universität Chemnitz, Fakultät für Naturwissenschaften, Institut für Chemie, Professur Anorganische Chemie, 09107 Chemnitz, Germany

Supporting information for this article is available on the WWW under <http://dx.doi.org/10.1002/ejic.201300889>.

$\text{Bi}_2\text{O}_3$  nanoparticles was chosen as a model reaction.<sup>[8]</sup> For comparison, the photocatalytic activities of **3** in solution (DMF/ $\text{H}_2\text{O}$ ) and of suspensions of **1–4** in water under visible-light irradiation and for cluster **3** also under UV/Vis conditions were determined. The syntheses and characterization of compounds **2–4** were reported recently; the bismuth oxido cluster **1** is reported here for the first time. The latter was obtained upon testing the influence of a variety of crystallization modulators on the hydrolysis behavior of bismuth nitrate.

## Results and Discussion

### Studies on the Hydrolysis of Bismuth(III) Nitrate

The addition of sodium methacrylate (NaOMc) to a solution of  $[\text{Bi}_6\text{O}_4(\text{OH})_4(\text{NO}_3)_6]\cdot\text{H}_2\text{O}$ <sup>[3a]</sup> (**2**) in DMSO resulted in the formation of  $[\text{Bi}_{38}\text{O}_{45}(\text{OMc})_{24}(\text{DMSO})_9]\cdot 2\text{DMSO}\cdot 7\text{H}_2\text{O}$  (**4**),<sup>[6b]</sup> whereas  $[\{\text{Bi}_{38}\text{O}_{45}(\text{NO}_3)_{24}(\text{DMSO})_{26}\}\cdot 2\text{DMSO}][\{\text{Bi}_{38}\text{O}_{45}(\text{NO}_3)_{24}(\text{DMSO})_{24}\}\cdot 0.5\text{DMSO}]$ <sup>[5]</sup> (**3**) is obtained when  $\text{Bi}(\text{NO}_3)_3\cdot 5\text{H}_2\text{O}$  was used instead of the hexanuclear bismuth oxido cluster **2**. In the latter case, the additive NaOMc modulates the crystallization behavior but is not incorporated into the final material. Without addition of NaOMc, the bismuth complex  $[\text{Bi}(\text{NO}_3)_3(\text{DMSO})_3]$ <sup>[11]</sup> was observed.<sup>[5]</sup> These previously reported results demonstrate that additives are essential to obtain bismuth oxido clusters of high nuclearity from bismuth nitrate solutions, but the role of the modulators is still unclear. The basicity of additives such as NaOMc might be one of the main aspects that influences condensation reactions to give  $[\text{Bi}_{38}\text{O}_{45}]^{24+}$  species. We have thus investigated the influence of additives with different  $\text{p}K_{\text{b}}$  values<sup>[12]</sup> such as sodium acetate, sodium benzoate, sodium formiate, sodium chloroacetate, sodium dichloroacetate, and sodium trichloroacetate on the condensation reaction of bismuth nitrate in DMSO. After slow evaporation of the solvent, crystalline materials were observed in all cases that were shown to be mainly  $[\text{Bi}(\text{NO}_3)_3(\text{DMSO})_3]$  if the sodium salts of chloroacetate, dichloroacetate, and trichloroacetate are added (Figure 1), whereas the addition of sodium formiate and sodium acetate gave  $[\{\text{Bi}_{38}\text{O}_{45}(\text{NO}_3)_{24}(\text{DMSO})_{26}\}\cdot 2\text{DMSO}][\{\text{Bi}_{38}\text{O}_{45}(\text{NO}_3)_{24}(\text{DMSO})_{24}\}\cdot 0.5\text{DMSO}]$  (**3**), similar to the results observed upon addition of NaOMc.<sup>[5]</sup> The identity of compound **3** was confirmed by single-crystal and powder X-ray diffraction. In contrast, the data obtained for crystals formed upon addition of sodium benzoate did not fit to any reported data on bismuth compounds (Figure 1), and single-crystal X-ray diffraction analysis revealed the formation of a novel cluster with a mixed ligand shell,  $[\{\text{Bi}_{38}\text{O}_{45}(\text{NO}_3)_{20}(\text{OBz})_4(\text{DMSO})_{24}\}\cdot 4\text{DMSO}][\{\text{Bi}_{38}\text{O}_{45}(\text{NO}_3)_{24}(\text{DMSO})_{26}\}\cdot 4\text{DMSO}]$  (**1**) (OBz = benzoate).

Compound **1** crystallizes in the monoclinic space group  $P2_1/c$  with cell parameters of  $a = 35.8728(12)$  Å,  $b = 20.2750(5)$  Å,  $c = 34.8624(11)$  Å, and  $\beta = 111.797(4)^\circ$ , and two crystallographically independent molecules in the asymmetric unit, both with different substitution patterns at the  $[\text{Bi}_{38}\text{O}_{45}]^{24+}$  core: (1)  $[\text{Bi}_{38}\text{O}_{45}(\text{NO}_3)_{20}(\text{OBz})_4$

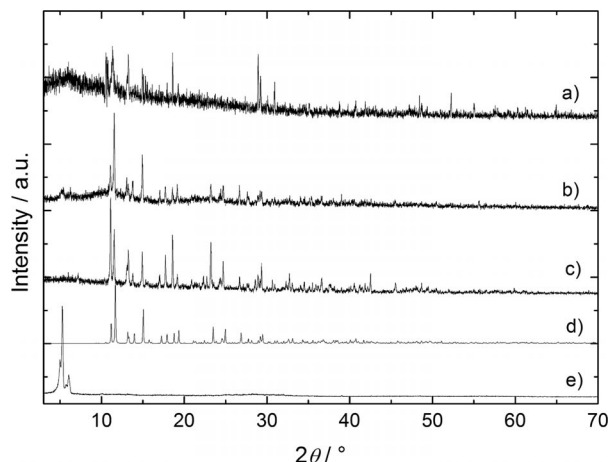


Figure 1. Powder X-ray diffraction patterns obtained for crystals after slow evaporation of DMSO from the reaction mixture:  $\text{Bi}(\text{NO}_3)_3\cdot 5\text{H}_2\text{O}$  with (a) sodium trichloroacetate, (b) sodium dichloroacetate, and (c) sodium chloroacetate, respectively. (d) Calculated powder pattern on the basis of single-crystal X-ray data of  $[\text{Bi}(\text{NO}_3)_3(\text{DMSO})_3]$ .<sup>[11]</sup> (e) The measured PXRD pattern of crystals of the novel bismuth oxido cluster **1**.

$(\text{DMSO})_{24}] \cdot 4\text{DMSO}$  (**1a**·4DMSO) and (2)  $[\text{Bi}_{38}\text{O}_{45}(\text{NO}_3)_{24}(\text{DMSO})_{26}] \cdot 4\text{DMSO}$  (**1b**·4DMSO) (Figure 2). The crystalline material is a cocrystal of a  $\{\text{Bi}_{38}\}$  nitrate cluster, as observed previously, and a  $\{\text{Bi}_{38}\}$  cluster in which four nitrates are substituted by benzoate.<sup>[5]</sup> As reported earlier, a  $\mu_6$ -coordinated oxygen atom occupies an octahedral void in the center of the  $[\text{Bi}_{38}\text{O}_{45}]^{24+}$  core of both clusters [ $\text{Bi}-\text{O}$  **1a**: 2.5205(8)–2.6477(11) Å; **1b**: 2.5422(9)–2.5846(9) Å], and thus a  $[\text{Bi}_6\text{O}_9]$  unit represents the central motif, which is surrounded by twelve edge-sharing octahedral  $[\text{Bi}_6\text{O}_8]^{2+}$  units that form a nearly face-centered cubic lattice in which the tetrahedral voids are filled with oxygen atoms.

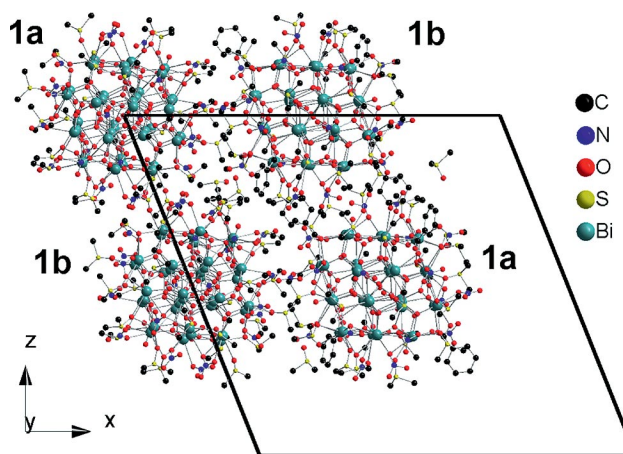


Figure 2. Cutout of the monoclinic unit cell of **1** displaying the packing of the two centrosymmetric bismuth oxido clusters  $[\text{Bi}_{38}\text{O}_{45}(\text{NO}_3)_{20}(\text{OBz})_4(\text{DMSO})_{24}] \cdot 4\text{DMSO}$  (**1a**·4DMSO) and  $[\text{Bi}_{38}\text{O}_{45}(\text{NO}_3)_{24}(\text{DMSO})_{26}] \cdot 4\text{DMSO}$  (**1b**·4DMSO). Hydrogen atoms are omitted for clarity.

In cluster **1a**, the  $[\text{Bi}_{38}\text{O}_{45}]^{24+}$  core is built up by 20  $\mu_3$ - and 24  $\mu_4$ -bridging oxygen atoms with Bi–O bond lengths in the range from 2.084(13) to 2.520(12) Å and 2.065(13) to

2.964(12) Å, respectively. In cluster **1b**, 16 oxygen atoms show a  $\mu_3$ -coordination, whereas 28 oxygen atoms build a  $\mu_4$ -coordination with Bi–O bond lengths of 2.089(12)–2.415(13) Å and 2.067(13)–2.905(11) Å, respectively. The coordination spheres of the bismuth atoms in **1** are built up by a varying number of anionic ligands and DMSO molecules. Thus, the coordination numbers of the bismuth atoms vary from 5 to 9 to result in triangular-based [3+ $x$ ] ( $x = 2–6$ ) and square-based [4+ $x$ ] ( $x = 1–5$ ) pyramids capped by a varying number of oxygen atoms ( $x$ ). Primary bonds with Bi–O bond lengths in the range from 2.065(13) to 2.489(11) Å constitute the base of the pyramids. The secondary bonds, which are suggested to result from the interaction of the HOMOs of the ligands with the  $\delta^*(\text{Bi–O})$  orbitals, range from 2.520(12) to 2.991(12) Å.<sup>[13]</sup> The distortion of the polyhedra is assigned to a stereochemically active lone pair at the bismuth atoms. The manifold coordination numbers of the bismuth atoms are also expressed by bismuth bond-valence parameters that vary from 2.48 to 3.54.<sup>[14]</sup> In **1a**·4DMSO, the coordination sphere of the bismuth atoms is built up by the coordination of four benzoates, 20 nitrates, and 24 DMSO molecules, and in addition four noncoordinated DMSO molecules are present in the crystal lattice (Figure 3). Two benzoates coordinate in a  $\mu_4$ -1 $\kappa O$ :2 $\kappa O$ :3 $\kappa O'$ :4 $\kappa O'$  mode [2.523(13)–2.97(3) Å] and two in a  $\mu_3$ -1 $\kappa O$ :2 $\kappa O$ :3 $\kappa O'$  mode [2.584(14)–2.742(12) Å], whereas four DMSO molecules show a monodentate [2.711(15)–2.897(14) Å] and 20 a bidentate [2.542(14)–2.946(13) Å] coordination through their oxygen atoms. Ten nitrate ligands exhibit a monodentate [2.77(2)–2.991(12) Å], six a  $\mu$ -1 $\kappa O$ :2 $\kappa O$ -type [2.730(19)–2.967(17) Å], two a  $\mu$ -1 $\kappa O$ :2 $\kappa O'$ -type [2.868(16)–2.923(18) Å], and two a 1 $\kappa^2 O, O'$ -type coordination [2.679(17)–2.847(17) Å]. Similar coordination modes of the ligands are observed in **1b**·4DMSO: Four

DMSO molecules are noncoordinated, eight coordinate in a monodentate fashion [2.719(15)–2.946(14) Å], and 18 bidentate [2.530(15)–2.938(15) Å] through their oxygen atoms to the [Bi<sub>38</sub>O<sub>45</sub>]<sup>24+</sup> core. Of the 24 coordinating nitrate ligands, four show a monodentate [2.738(14)–2.979(17) Å], ten a  $\mu$ -1 $\kappa O$ :2 $\kappa O$ -type [2.716(15)–2.976(19) Å], six a  $\mu$ -1 $\kappa O$ :2 $\kappa O'$ -type [2.694(19)–2.824(19) Å], and four a 1 $\kappa^2 O, O'$ -type coordination [2.670(16)–2.954(13) Å].

The [Bi<sub>38</sub>O<sub>45</sub>]<sup>24+</sup> cores of the cocrystal **1** composed of **1a** and **1b** are quite similar but not identical, as it is shown by a comparison of the atom positions of both bismuth oxido cores (Figure S1 in the Supporting Information). The only identical position is found for the  $\mu_6$ -coordinated oxygen atom in the center of both bismuth oxido clusters. A weighted root mean square deviation of 0.317 Å containing a maximum deviation of 0.847 Å is obtained for the differences of the oxygen atom positions in clusters **1a** and **1b**, the bismuth atom positions show a weighted root mean square deviation of 0.288 Å with a minimum deviation of 0.042 Å and a maximum deviation of 0.524 Å.

### Photocatalytic Investigations

Recently, heterobimetallic bismuth-containing clusters such as H<sub>3</sub>{[Bi(DMSO)<sub>3</sub>]<sub>4</sub>V<sub>13</sub>O<sub>40</sub>}, defined as “molecular bismuth vanadate”, have been demonstrated to be efficient photocatalysts in the visible-light region even though their absorption maximum is located below 300 nm and the absorption intensity clearly diminishes at wavelengths higher than 400 nm.<sup>[10]</sup> This report encouraged us to probe whether homometallic molecular bismuth oxido clusters, which we have been studying in recent years, exhibit photocatalytic activity as well. Here we focus on the novel bismuth oxido cluster [Bi<sub>38</sub>O<sub>45</sub>(NO<sub>3</sub>)<sub>20</sub>(OBz)<sub>4</sub>(DMSO)<sub>24</sub>·4DMSO][Bi<sub>38</sub>O<sub>45</sub>(NO<sub>3</sub>)<sub>24</sub>(DMSO)<sub>26</sub>·4DMSO] (**1**) and the previously reported clusters [Bi<sub>6</sub>O<sub>4</sub>(OH)<sub>4</sub>(NO<sub>3</sub>)<sub>6</sub>]·H<sub>2</sub>O<sup>[3a]</sup> (**2**), [Bi<sub>38</sub>O<sub>45</sub>(NO<sub>3</sub>)<sub>24</sub>(DMSO)<sub>26</sub>·2DMSO][Bi<sub>38</sub>O<sub>45</sub>(NO<sub>3</sub>)<sub>24</sub>(DMSO)<sub>24</sub>·0.5DMSO]<sup>[5]</sup> (**3**), and [Bi<sub>38</sub>O<sub>45</sub>(OMc)<sub>24</sub>(DMSO)<sub>9</sub>]·2DMSO·7H<sub>2</sub>O<sup>[6b]</sup> (**4**). The bismuth oxido clusters were tested as photocatalysts for rhodamine B (RhB) degradation under visible-light irradiation to evaluate the influence of the cluster size and the nature of the ligand shell. The latter aspect is of importance in developing model compounds to mimic bismuth oxide surfaces.

First, the bandgaps of clusters **1–4** were analyzed. On the basis of UV/Vis measurements in diffuse reflectance mode, the absorption edges and the bandgaps, which were calculated using Tauc plots,<sup>[15]</sup> were determined as 351 nm (3.61 eV) for **1**, 335 nm (3.76 eV) for **2**, and 346 nm (3.64 eV) for **3** and **4**, respectively (Figure 4 and Figure S2 in the Supporting Information). For comparison, the absorption edges were also determined for solutions in DMSO and DMF. As shown in Figure S3 of the Supporting Information, smaller absorption edges relative to the solid state were obtained, whereas a small shift to longer wavelengths was observed by changing the solvent from DMSO (**1**: 295 nm; **2**: 309 nm; **4**: 306 nm) to DMF (**1**:

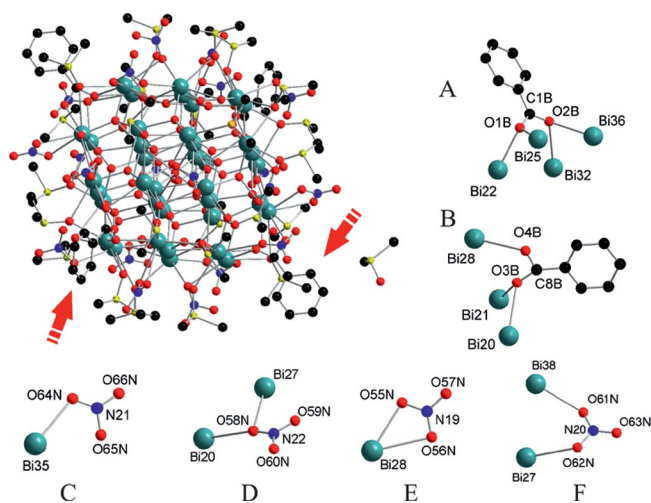


Figure 3. Ball-and-stick model of [Bi<sub>38</sub>O<sub>45</sub>(NO<sub>3</sub>)<sub>20</sub>(OBz)<sub>4</sub>(DMSO)<sub>24</sub>]<sup>24+</sup>·4DMSO (**1a**·4DMSO) and typical coordination modes (arrows show the coordination of the four benzoate ligands): (A)  $\mu_4$ -1 $\kappa O$ :2 $\kappa O$ :3 $\kappa O'$ :4 $\kappa O'$  mode, (B)  $\mu_3$ -1 $\kappa O$ :2 $\kappa O$ :3 $\kappa O'$  mode. The lower part represents the coordination of the nitrate ligands: (C) Monodentate, (D)  $\mu$ -1 $\kappa O$ :2 $\kappa O$  mode, (E) 1 $\kappa^2 O, O'$  mode, and (F)  $\mu$ -1 $\kappa O$ :2 $\kappa O'$  mode. Hydrogen atoms are omitted for clarity.

301 nm; **3**: 301 nm; **4**: 311 nm). Cluster **2** was measured solely in DMSO and cluster **3** in DMF due to low solubility in other solvents. As observed from the experiments, a response of the clusters with regard to photocatalysis is expected under UV light rather than under visible light irradiation. However, heterobimetallic bismuth-containing clusters, as mentioned above, also exhibit absorption band maxima in the UV/Vis region but show auspicious visible-light-induced photodegradation, for example, of patent blue V.<sup>[10]</sup> However, in most cases, photosensitizers such as [Ru(bpy)<sub>3</sub>]<sup>2+</sup> (bpy = 2,2'-bipyridine) are added to improve the visible-light photoactivity of the metal oxido clusters.<sup>[9a]</sup> Additionally, photocatalytic activity also depends on the model dyes that are used. RhB, used as the model dye in this study, shows a distinct chromophoric system that facilitates light absorption in the visible-light region. By interaction of RhB with a semiconductor, electron-transfer processes can be induced by irradiation with visible light, which results in *N*-deethylation processes of RhB even if the bandgap of the semiconductor is larger than 3.0 eV.<sup>[16]</sup> In addition to such photosensitization processes RhB can also be degraded with complete destruction of the chromophoric system as a result of the interaction with electron-hole pairs generated by excitation of the semiconductor with light irradiation.<sup>[16b]</sup>

One interesting aspect for photocatalysts based on molecular materials relative to bulk metal oxides is their solubility in organic solvents, which might offer the possibility to perform photocatalysis in homogeneous solution. To elucidate this possibility, the highly soluble bismuth oxido cluster **3** (40 mg) was dissolved in dimethylformamide (20 mL) and was mixed with an aqueous rhodamine B (RhB) solution (20 mL,  $2 \times 10^{-5}$  M). These conditions were chosen because they are comparable to those in our previously reported heterogeneous photocatalytic experiments using  $\beta$ -Bi<sub>2</sub>O<sub>3</sub> nanoparticles.<sup>[8]</sup> After dissolution, the homogeneous mixture was illuminated with visible light ( $400 \text{ nm} \leq \lambda \leq 700 \text{ nm}$ ), and the photocatalytic activity was monitored by in situ UV/Vis measurements. However, in this experiment, a negligible degradation rate of  $1.21 \times 10^{-6} \text{ s}^{-1}$  (1.3% decomposition after 150 min) was observed, and we conclude that our molecular bismuth oxido clusters are almost inactive, as expected from the size of the bandgaps (Figure S4 in the Supporting Information). The use of UV/Vis light gave a slightly higher decomposition rate of  $4.10 \times 10^{-6} \text{ s}^{-1}$  (3.5% decomposition after 150 min; Figure S5 in the Supporting Information). The negligible increase in the decomposition rate might be attributed to the instrumental light source, which only provides light with wavelengths longer than 370 nm. Thus, the bismuth oxido cluster is not directly excited and the higher decomposition rate is a result of the higher energy of the light source, which is provided as a result of the removal of the UV cut-off filter. For further investigations, another photoreactor with a 160 W mercury-vapor lamp that provided light above 250 nm was used (Figure S6 in the Supporting Information). In this experiment, a decomposition rate of  $4.71 \times 10^{-6} \text{ s}^{-1}$  after 150 min was obtained (4.3% decompo-

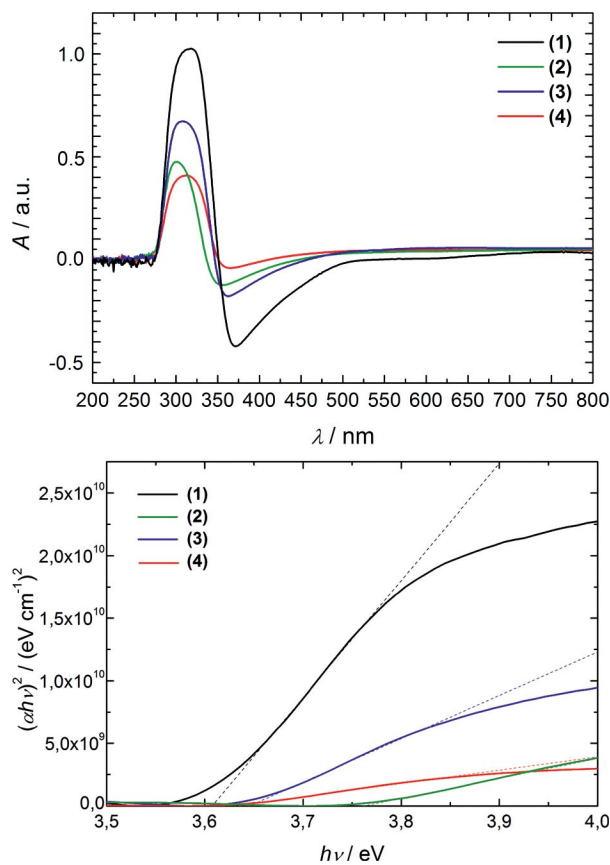


Figure 4. Normalized UV/Vis diffuse reflectance spectra (top) and  $(ah\nu)^2$  versus  $h\nu$  curves (bottom) of bismuth oxido clusters **1**, **2**, **3**, and **4**. The single UV/Vis diffuse reflectance spectra are given in Figure S2 of the Supporting Information.

sition), which is still low-level. The low performance as a result of decomposition of the cluster is excluded. We have demonstrated by several methods (including ESI-MS) that cluster **3** is stable in diverse solvents.<sup>[6a,17]</sup> In addition, cluster **3** was dissolved in a DMF/H<sub>2</sub>O mixture (1:1) and after evaporation of the solvent a crystalline material was obtained, which indicates that the bismuth oxido core is still intact as demonstrated by typical diffraction peaks centered at  $4.93$  and  $5.73^\circ$  ( $2\theta$ ) (Figure S7 in the Supporting Information).<sup>[6c,17]</sup> The main reason for the low activity seems to be that RhB does not adsorb effectively to the cluster surface.

In a typical heterogeneous photocatalytic experiment, the bismuth oxido clusters (40 mg) were dispersed in an aqueous RhB solution (40 mL,  $10^{-5}$  M). Thus, dynamic light scattering (DLS) experiments in water were made for all tested bismuth oxido clusters to investigate their behavior in aqueous suspensions. Values of  $(2.2 \pm 0.8)$  and  $(17.1 \pm 14.3)$  nm (**1**),  $(2.3 \pm 0.5)$  and  $(14.4 \pm 4.8)$  nm (**2**),  $(2.5 \pm 0.5)$  and  $(10.9 \pm 4.4)$  nm (**3**), as well as  $(3.1 \pm 0.7)$  and  $(11.5 \pm 5.3)$  nm (**4**) were obtained (Figures S6–S9 in the Supporting Information). As a result of agglomeration, bimodal distributions are obtained for all bismuth oxido clusters, but the tendency to form agglomerates is less distinct for cluster **2**. Prior to irradiation, the samples were stirred

in the dark to establish the adsorption/desorption equilibrium ( $-30 \text{ min} \leq t \leq 0 \text{ min}$ ). A change in intensity of the characteristic RhB absorption band during this period shows that RhB is partially adsorbed at the bismuth oxido cluster surfaces; the large clusters **1** (13%), **3** (16%), and **4** (27%) adsorb a significant amount of the initially present RhB (Figure 5), whereas adsorption by cluster **2** and the commercially available  $\text{Bi}(\text{NO}_3)_3 \cdot 5\text{H}_2\text{O}$  is negligible ( $<1\%$ ).

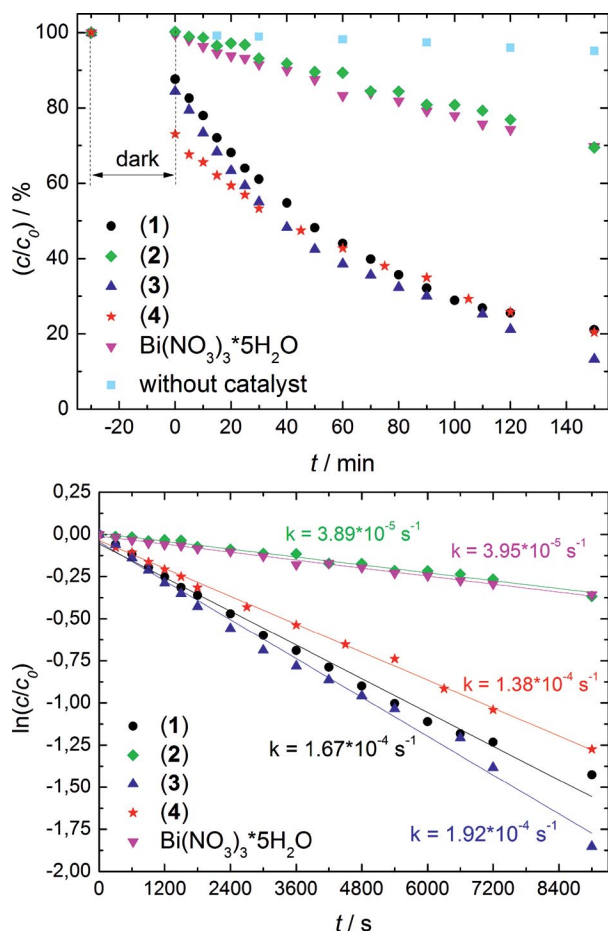


Figure 5. Time-dependent conversion (top) and semilogarithmic plots (bottom) of the photodegradation of an aqueous RhB solution ( $10^{-5} \text{ M}$ ) under visible light irradiation ( $t > 0 \text{ min}$ ) using bismuth oxido clusters **1–4** and  $\text{Bi}(\text{NO}_3)_3 \cdot 5\text{H}_2\text{O}$  as photocatalysts;  $t < 0 \text{ min}$  shows the adsorption behavior of the samples towards RhB.

Starting the irradiation using visible light ( $t > 0 \text{ min}$ ) immediately initiates photodegradation processes. All of the tested bismuth oxido clusters show photocatalytic activity, whereas in the absence of a photocatalyst a negligible decomposition of RhB within 150 min ( $<5\%$ ) is observed. As shown in Figure 5, the photocatalytic degradation in the presence of the bismuth oxido clusters follows pseudo-first-order reaction kinetics and hence the reaction rate constants were determined from the slope of the linear functions obtained by semilogarithmic plots of  $\ln(c/c_0)$  versus time. The highest photocatalytic activity is observed for the bismuth oxido cluster **3**, which decomposes 87% of RhB within 150 min with a reaction rate constant of

$1.92 \times 10^{-4} \text{ s}^{-1}$ . Under identical conditions, the samples **1**, **2**, and **4** decompose 79 ( $1.67 \times 10^{-4} \text{ s}^{-1}$ ), 31 ( $3.89 \times 10^{-5} \text{ s}^{-1}$ ), and 80% ( $1.38 \times 10^{-4} \text{ s}^{-1}$ ) of RhB, respectively. The use of commercially available  $\text{Bi}(\text{NO}_3)_3 \cdot 5\text{H}_2\text{O}$  shows decomposition of approximately 30% of RhB with a reaction rate constant of  $3.95 \times 10^{-5} \text{ s}^{-1}$ , which is comparable to the performance of the hexanuclear cluster **2**. However, all of the tested compounds show a lower photocatalytic activity than  $\beta\text{-Bi}_2\text{O}_3$  nanoparticles as prepared starting from bismuth oxido clusters.<sup>[8]</sup> A closer look at the chemical composition of the bismuth oxido clusters tested show that, in the case of cluster **2**, DMSO is missing as coordinated solvent. Thus, the photocatalytic experiment using cluster **2** as photocatalyst was repeated, and 9 mg of DMSO was added to give a similar amount of DMSO molecules per bismuth atom relative to the other bismuth oxido clusters tested. However, no increase in the photocatalytic performance was observed ( $k = 3.81 \times 10^{-5} \text{ s}^{-1}$ ; Figure S12 in the Supporting Information) and thus any influence of DMSO is excluded. A higher nuclearity of bismuth oxido clusters is associated with an increasing photocatalytic activity, and hence higher decomposition rates compared to cluster **2** and  $\text{Bi}(\text{NO}_3)_3 \cdot 5\text{H}_2\text{O}$  are obtained, respectively. This is most likely attributed to agglomeration in aqueous media, as shown by DLS experiments, as well as to significant RhB adsorption, which is much more distinct for bismuth oxido clusters **1**, **3**, and **4**. Furthermore, higher-nuclearity bismuth oxido clusters are composed of a larger number of  $[\text{Bi}_6\text{O}_{8+x}]^{2(1-x)+}$  units ( $x = 0, 1$ ), which results in a closer structural relationship to the photocatalytically active  $\beta\text{-Bi}_2\text{O}_3$ .<sup>[7,8]</sup> Powder X-ray diffraction (PXRD) analyses after photocatalytic degradation experiments have shown that the crystalline materials were transformed to give powders of lower crystallinity, but they are not fully amorphous (Figure S13 in the Supporting Information). However, the loss of crystallinity during photodegradation is attributed not to photocorrosion but to ligand exchange in aqueous media, which was similarly observed by simply stirring the crystalline materials in water in control experiments. Nevertheless, the PXRD patterns indicate that the bismuth oxido cluster cores are not destroyed. This assumption was additionally proven by solid-state UV/Vis measurements, which show no change for the absorption edges of clusters **1–4** after their use in a photocatalytic process (Figure S14 in the Supporting Information).

To shed some more light on the degradation process of RhB, further photocatalytic experiments were performed. First, a RhB solution that contained the best photocatalyst, cluster **3**, was irradiated with UV/Vis light to probe the photocatalytic performance under standard procedures. After 150 min of irradiation, approximately 95% of the initial RhB amount was degraded ( $k = 3.29 \times 10^{-4} \text{ s}^{-1}$ ; Figure S15 in the Supporting Information). Thus, the photocatalytic performance was approximately doubled (a factor of 1.7) relative to the previous investigations in which visible light is used exclusively. The irradiation with UV/Vis light allows direct excitation of the bismuth oxido cluster, which results in higher decomposition rates. Thus, direct and indirect

photocatalytic processes might be present. Further UV/Vis experiments were performed to identify crucial processes in RhB degradation on the surface of bismuth oxido clusters. As shown by way of example in Figure 6 for a suspension of cluster **3**, no significant blueshift of the absorption band of RhB is observed in all degradation experiments, which is indicative of a fast decomposition of the chromophore system to finally give CO<sub>2</sub> and water.<sup>[18]</sup> Another possible degradation process that occurs by means of photooxidation induces stepwise deethylation of the *N,N,N',N'*-tetraethylrhodamine, which results in a sequential blueshift of the characteristic RhB absorption band ( $\lambda_{\text{max}} = 554 \text{ nm}$ ). This is a result of the stepwise formation of the degradation products *N,N,N'*-triethylrhodamine ( $\lambda_{\text{max}} = 539 \text{ nm}$ ), *N,N'*-diethylrhodamine ( $\lambda_{\text{max}} = 522 \text{ nm}$ ), *N*-ethylrhodamine ( $\lambda_{\text{max}} = 510 \text{ nm}$ ), and rhodamine ( $\lambda_{\text{max}} = 498 \text{ nm}$ ).<sup>[16b]</sup> However, the absence of the blueshift in solution during RhB decomposition might not fully reflect the degradation process of RhB that typically occurs at the surface of a heterogeneous photocatalyst. To study the photooxidation process at the cluster surface, the photodegradation of adsorbed RhB was studied under visible light and for comparison also under UV/Vis conditions. A small amount of RhB (1  $\mu\text{M}$ ) was adsorbed on the surface of cluster **3** (Figure 7), and UV/Vis measurements in diffuse reflectance mode were recorded. A decrease in intensity of the RhB absorption band along with a sequential blueshift to 510 nm within 60 min during continuous irradiation with the instrument light source (100 W) was observed. A similar behavior was obtained under visible-light conditions, but a smaller amount of RhB was decomposed than in the experiment under UV/Vis conditions. The lower activity results from the lower energy that is available for the photodegradation process due to the absorption of light by the UV cutoff filter. Additionally, the bismuth oxido cluster is not directly excited under visible-light conditions as a result of the bandgap of 3.64 eV, therefore the degradation of RhB must be induced by photosensitization. In this process, one electron of the chromophoric system of RhB is excited by absorption of visible light, which is then transferred to the conduction band of the photocatalyst.<sup>[16a]</sup> The electron is removed from the conduction band by interaction with oxygen to give a superoxide radical, and a double bond at RhB is formed by separation of a proton. Several repetitions of these processes lead to *N*-deethylation of RhB, which results in ongoing degradation. Thus, direct interactions of RhB with the surface of a photocatalyst is important prior to inducing degradation. Direct excitation of the photocatalyst by light to generate electron holes is not necessary. These processes have been reported previously.<sup>[16]</sup> The experiments presented here show that *N,N,N'*-triethylrhodamine and *N,N'*-diethylrhodamine are continuously formed (as a result of an ongoing deethylation process of RhB at the surface of the bismuth oxido cluster **3**) regardless of whether UV/Vis or visible light is used. The results therefore indicate that photosensitization processes are predominant in degradation of RhB with bismuth oxido clusters as photocatalysts. It is worth noting that similar experiments using MgO instead of the

clusters or pure RhB did result in very low photodecomposition rates without any blueshift (Figures S16 and S17 in the Supporting Information). Thus we conclude that the photodegradation process of RhB occurs preferentially at heterogeneous surfaces of the bismuth-containing colloids under UV/Vis as well as visible conditions and is comparable to the process as reported for bismuth oxide nanoparticles.<sup>[8]</sup> This explains the low activity of **2** and also of **3** in solution, both of which lack strong adsorption of RhB.

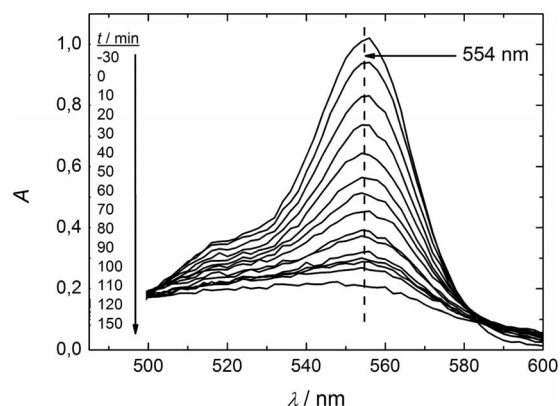


Figure 6. UV/Vis spectra of the photodegradation of RhB using bismuth oxido cluster **3** as dispersed photocatalyst in water ( $t = -30 \text{ min}$ : starting stirring in the dark;  $t = 0 \text{ min}$ : starting irradiation with visible light).

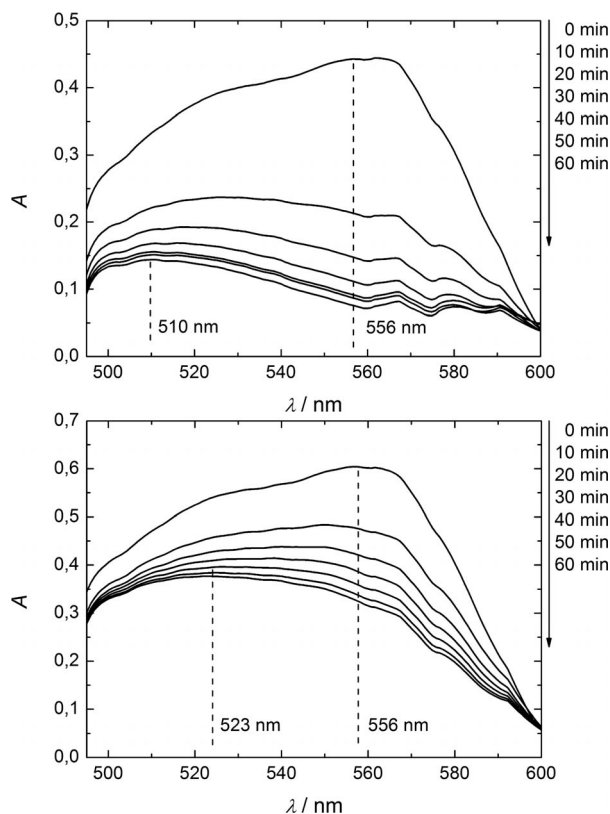


Figure 7. Diffuse reflectance spectra of solid bismuth oxido cluster **3** with adsorbed RhB under UV/Vis (top) and visible light irradiation (bottom).

## Conclusion

The investigations presented here have shown that additives play an important role in the formation of bismuth oxido clusters starting from solutions of bismuth(III) nitrate in DMSO. We have demonstrated the influence of sodium acetate, sodium benzoate, sodium formiate, sodium chloroacetate, sodium dichloroacetate, and sodium trichloroacetate. Depending on the  $pK_b$  values of the additives, the formation of  $[\text{Bi}(\text{NO}_3)_3(\text{DMSO})_3]$  ( $pK_b \geq 11.2$ ) and  $[\{\text{Bi}_{38}\text{O}_{45}(\text{NO}_3)_{24}(\text{DMSO})_{26}\} \cdot 2\text{DMSO}][\{\text{Bi}_{38}\text{O}_{45}(\text{NO}_3)_{24}(\text{DMSO})_{24}\} \cdot 0.5\text{DMSO}]^{[5]}$  ( $pK_b \leq 10.3$ ) was observed. However, in the case of sodium benzoate ( $pK_b$  9.8), four nitrate ligands were substituted for four benzoates, which resulted in the formation of a cocrystal of similar  $\{\text{Bi}_{38}\}$  clusters,  $[\{\text{Bi}_{38}\text{O}_{45}(\text{NO}_3)_{20}(\text{OBz})_4(\text{DMSO})_{24}\} \cdot 4\text{DMSO}][\{\text{Bi}_{38}\text{O}_{45}(\text{NO}_3)_{24}(\text{DMSO})_{26}\} \cdot 4\text{DMSO}]$  (**1**). The photocatalytic investigations on the degradation of rhodamine B under visible-light irradiation have shown the promising activity of colloidal suspensions of the bismuth oxido clusters **1**,  $[\{\text{Bi}_{38}\text{O}_{45}(\text{NO}_3)_{24}(\text{DMSO})_{26}\} \cdot 2\text{DMSO}][\{\text{Bi}_{38}\text{O}_{45}(\text{NO}_3)_{24}(\text{DMSO})_{24}\} \cdot 0.5\text{DMSO}]^{[5]}$  (**3**), and  $[\text{Bi}_{38}\text{O}_{45}(\text{OMc})_{24}(\text{DMSO})_9] \cdot 2\text{DMSO} \cdot 7\text{H}_2\text{O}^{[6b]}$  (**4**), but only minor activity for  $[\text{Bi}_6\text{O}_4(\text{OH})_4(\text{NO}_3)_6] \cdot \text{H}_2\text{O}^{[3a]}$  (**2**). The highest degradation rate using visible light irradiation was obtained for compound **3**, which decomposes approximately 87% of a  $10^{-5}$  M aqueous solution of RhB within 150 min with a reaction rate constant of  $1.92 \times 10^{-4} \text{ s}^{-1}$ , whereas under homogeneous conditions a negligible photocatalytic activity was observed. Furthermore, the studies have shown that the photocatalytic degradation of RhB under visible-light irradiation by using bismuth oxido clusters as photocatalysts preferentially occurs through indirect photocatalytic processes and that adsorption properties play an important role. Finally, we postulate that bismuth oxido clusters might serve as model compounds to mimic bismuth oxide surfaces in photocatalytic processes, especially when the indirect photocatalytic process is favored.

## Experimental Section

**General:** PXRD patterns were measured with a STOE-STADI-P diffractometer using  $\text{Cu-K}\alpha$  radiation (40 kV, 40 mA) and a Ge(111) monochromator. The decomposition points were determined with a Büchi melting apparatus "Melting Point B-540" and are uncorrected. The data set for the single-crystal X-ray diffraction study was collected by using  $\text{Mo-K}\alpha$  radiation (0.71073 Å) with an Oxford Gemini S diffractometer at 110 K. All calculations were performed using the SHELXTL program.<sup>[19]</sup> The structures were solved by direct methods and refined by full-matrix least-squares on  $F^2$ . Diffuse reflectance UV/Vis spectroscopy was performed with a single-beam simultaneous spectrometer MCS 400 (Co. Carl Zeiss Jena GmbH). The UV and visible-light radiation were generated with a CLD 300 deuterium lamp and a CLX 11 xenon lamp, respectively. For in situ UV/Vis measurements, which were carried out to examine the photocatalytic activity, an Agilent Cary 60 UV/Vis spectrometer (Co. Agilent Technologies) equipped with fiber optics was used. DLS was performed with a Viscotek model 802 equipped with a laser diode that provided light with a wavelength

of 830 nm. In every DLS experiment a concentration of  $1 \text{ g L}^{-1}$  was used.

Bismuth oxido clusters **2**,<sup>[3a]</sup> **3**,<sup>[5]</sup> and **4**<sup>[6b]</sup> were synthesized according to the literature.

**General Procedure for Hydrolysis of  $\text{Bi}(\text{NO}_3)_3$  in the Presence of Additives:** A suspension of  $\text{Bi}(\text{NO}_3)_3 \cdot 5\text{H}_2\text{O}$  (2.1 g, 4.25 mmol) in DMSO (10 mL) was stirred at  $80^\circ\text{C}$  to give a colorless solution. An appropriate amount (4.25 mmol) of the investigated additive was added in one portion, then the reaction mixture was stirred at  $80^\circ\text{C}$  overnight and filtered. The filtrate was kept under ambient conditions for crystallization.

**Synthesis of  $[\{\text{Bi}_{38}\text{O}_{45}(\text{NO}_3)_{20}(\text{OBz})_4(\text{DMSO})_{24}\} \cdot 4\text{DMSO}][\{\text{Bi}_{38}\text{O}_{45}(\text{NO}_3)_{24}(\text{DMSO})_{26}\} \cdot 4\text{DMSO}]$  (**1**):** By using the above-described procedure and sodium benzoate (0.6 g, 4.25 mmol) as additive, colorless crystals of compound **1** (0.4 g, 28%) were obtained, m.p.  $>200^\circ\text{C}$  decomp. IR:  $\tilde{\nu} = 3436$  (w, br.), 3008 (w), 2923 (w), 1603 (w), 1509 (m), 1472 (s), 1441 (s), 1401 (s), 1312 (m), 1268 (s), 1172 (m), 1072 (w), 1018 (s), 998 (s), 978 (s), 925 (s), 858 (s), 812 (m), 718 (s), 685 (s), 431 (w), 400 (s)  $\text{cm}^{-1}$ .  $\text{Bi}_{76}\text{C}_{144}\text{H}_{368}\text{O}_{288}\text{N}_{44}\text{S}_{58}$  (25066.78  $\text{g mol}^{-1}$ ): calcd. C 6.9, H 1.5, N 2.5; found C 7.0, H 1.6, N 2.5.

**Crystal Data:**  $\text{C}_{138}\text{H}_{358}\text{Bi}_{76}\text{N}_{44}\text{O}_{288}\text{S}_{58}$ ,  $M_r = 24904.53 \text{ g mol}^{-1}$ , crystal size  $0.3 \times 0.2 \times 0.2 \text{ mm}^3$ , monoclinic, space group  $P2_1/c$ ,  $Z = 2$ ,  $a = 35.8728(12) \text{ \AA}$ ,  $b = 20.2750(5) \text{ \AA}$ ,  $c = 34.8624(11) \text{ \AA}$ ,  $\beta = 111.797(4)^\circ$ ,  $V = 23543.3(12) \text{ \AA}^3$ ,  $D_{\text{calcd.}} = 3.536 \text{ g cm}^{-3}$ ,  $F(000) = 22160$ ,  $\mu(\text{Mo-K}\alpha) = 28.629 \text{ mm}^{-1}$ ,  $T = 293 \text{ K}$ ,  $2.92 < 2\theta < 25.00$ , completeness to  $2\theta$ : 99.4%. Max./min. residual electron density:  $3.852/-3.337 \text{ e \AA}^{-3}$ . A total of 111370 reflections collected, 41216 reflections were independent ( $R_{\text{int}} = 0.0878$ ). Final  $R_1 = 0.0524$  [ $I > 2\sigma(I)$ ] and  $wR_2 = 0.1067$  (all data).

CCDC-947073 contains the supplementary crystallographic data for this paper. These data can be obtained free of charge from The Cambridge Crystallographic Data Centre via [www.ccdc.cam.ac.uk/data\\_request/cif](http://www.ccdc.cam.ac.uk/data_request/cif).

**Photocatalytic Tests:** In a typical photodegradation experiment, an aqueous solution (40 mL) of  $1 \times 10^{-5}$  M rhodamine B dye (RhB) and the as-prepared samples (40 mg) in a water-cooled glass reactor ( $15^\circ\text{C}$ ) were used. After the suspension was stirred in the dark for 30 min to establish the adsorption/desorption equilibrium, irradiation with a 300 W xenon lamp (Cermax VQTM ME300BF, Co. Perkin–Elmer) equipped with a hot mirror filter ( $\lambda \leq 700 \text{ nm}$ ) and a UV cutoff filter ( $\lambda \geq 420 \text{ nm}$ , GG420, Co. Schott) to provide visible light was started. The effective irradiation area of the suspension was  $4.52 \text{ cm}^2$  (approx. 25% of the reactor area). The photocatalytic degradation was investigated by in situ UV/Vis measurements. Therefore stirring was stopped for 10 s and darkening of the light beam was achieved by the addition of a cover. The measurements were carried out up to a maximum time of 150 min (up to 30 min with a 5 min interval; up to 120 min with a 10 min interval). The photocatalytic degradation rates were determined by calculating the mathematical area under the characteristic UV/Vis absorption bands of RhB. In some extra reference experiments, the above-mentioned UV cutoff filter was removed and a 160 W mercury vapor lamp (TQ 150 EXKLUSIV UVCP, Co. Heraeus Noblelight GmbH) was used as light source.

**Supporting Information** (see footnote on the first page of this article): It contains DLS data, UV/Vis spectra, data of photocatalytic degradation experiments, powder X-ray diffraction patterns, and a structural comparison of the two  $[\text{Bi}_{38}\text{O}_{45}]^{24+}$  cores in **1**.

## Acknowledgments

The authors thank Prof. Dr. Stefan Spange for access to diffuse reflectance UV/Vis spectroscopy and Janine Fritzsich for performing CHN analyses. We gratefully acknowledge the financial support of this work by the Deutsche Forschungsgemeinschaft (DFG) (SPP1415) and the Fonds der Chemischen Industrie (FCI).

- [1] a) S. Serefis, *Arch. Dermatol. Syph.* **1934**, *171*, 1–98; b) P. J. Sadler, H. Y. Li, H. Z. Sun, *Coord. Chem. Rev.* **1999**, *185–6*, 689–709; c) N. Yang, H. Sun, *Coord. Chem. Rev.* **2007**, *251*, 2354–2366; d) H. Ippen, *Hautarzt* **1997**, *48*, 424–424; e) M. W. Whitehead, R. H. Phillips, C. E. Sieniawska, H. T. Delves, P. T. Seed, R. P. H. Thompson, J. J. Powell, *Helicobacter* **2000**, *5*, 169–175.
- [2] a) Y. M. Yukhin, T. V. Daminova, L. I. Afonina, B. B. Bokhonov, O. A. Logutenko, A. I. Aparnev, K. Y. Mikhailov, T. A. Udalova, V. I. Evseenko, *Chem. Sustainable Dev.* **2004**, *12*, 395–401; b) G. Gattow, D. Schott, *Z. Anorg. Allg. Chem.* **1963**, *324*, 31–47; c) B. S. Brcic, D. Kolar, F. Lazarini, M. Malesic, *Monatsh. Chem.* **1973**, *104*, 365–375.
- [3] a) F. Lazarini, *Acta Crystallogr., Sect. B* **1979**, *35*, 448–450; b) F. Lazarini, *Cryst. Struct. Commun.* **1979**, *8*, 69–74; c) F. Lazarini, *Acta Crystallogr., Sect. B* **1978**, *34*, 3169–3173; d) B. Liu, W. Zhou, Z. Zhou, X. Zhang, *Inorg. Chem. Commun.* **2007**, *10*, 1145–1148; e) A. N. Christensen, B. Lebeck, *Dalton Trans.* **2012**, *41*, 1971–1980.
- [4] K. H. Tytko, *Chem. Unserer Zeit* **1979**, *13*, 184–194.
- [5] L. Miersch, T. Rüffer, M. Schlesinger, H. Lang, M. Mehring, *Inorg. Chem.* **2012**, *51*, 9376–9384.
- [6] a) L. Miersch, M. Schlesinger, R. W. Troff, C. A. Schalley, T. Rüffer, H. Lang, D. Zahn, M. Mehring, *Chem. Eur. J.* **2011**, *17*, 6985–6990; b) L. Miersch, T. Rüffer, M. Mehring, *Chem. Commun.* **2011**, *47*, 6353–6355; c) D. Mansfeld, L. Miersch, T. Rüffer, D. Schaarschmidt, H. Lang, T. Böhle, R. W. Troff, C. A. Schalley, J. Müller, M. Mehring, *Chem. Eur. J.* **2011**, *17*, 14805–14810; d) M. Schlesinger, L. Miersch, T. Rüffer, H. Lang, M. Mehring, *Main Group Met. Chem.* **2013**, *36*, 11–19; e) P. C. Andrews, G. B. Deacon, C. M. Forsyth, P. C. Junk, I. Kumar, M. Maguire, *Angew. Chem.* **2006**, *118*, 5766; *Angew. Chem. Int. Ed.* **2006**, *45*, 5638–5642; f) P. C. Andrews, M. Busse, G. B. Deacon, R. L. Ferrero, P. C. Junk, J. G. Maclellan, A. Vom, *Dalton Trans.* **2012**, *41*, 11798–11806; g) E. V. Dikarev, H. Zhang, B. Li, *Angew. Chem.* **2006**, *118*, 5574; *Angew. Chem. Int. Ed.* **2006**, *45*, 5448–5451; h) V. Andre, A. Hardeman, I. Halasz, R. S. Stein, G. J. Jackson, D. G. Reid, M. J. Duer, C. Curfs, M. T. Duarte, T. Friscic, *Angew. Chem.* **2011**, *123*, 8004; *Angew. Chem. Int. Ed.* **2011**, *50*, 7858–7861.
- [7] M. Mehring, *Coord. Chem. Rev.* **2007**, *251*, 974–1006.
- [8] a) M. Schlesinger, S. Schulze, M. Hietschold, M. Mehring, *Dalton Trans.* **2013**, *42*, 1047–1056; b) M. Schlesinger, M. Weber, S. Schulze, M. Hietschold, M. Mehring, *ChemistryOpen* **2013**, *2*, 146–155.
- [9] a) C. Streb, *Dalton Trans.* **2012**, *41*, 1651–1659; b) C. L. Hill, *Comprehensive Coord. Chem. II* **2003**, *4*, 679–759; c) A. Hiskia, A. Mylonas, E. Papaconstantinou, *Chem. Soc. Rev.* **2001**, *30*, 62–69.
- [10] J. Tucher, L. C. Nye, I. Ivanovic-Burmazovic, A. Notarnicola, C. Streb, *Chem. Eur. J.* **2012**, *18*, 10949–10953.
- [11] L. J. Barbour, S. J. Belfield, P. C. Junk, M. K. Smith, *Aust. J. Chem.* **1998**, *51*, 337–342.
- [12]  $pK_b$  values in water: sodium methacrylate 9.4; sodium acetate 9.4; sodium bezoate 9.8; sodium formiate 10.3; sodium chloroacetate 11.2; sodium dichloroacetate 12.47; sodium trichloroacetate 13.3.
- [13] N. C. Norman, *Chemistry of Arsenic, Antimony and Bismuth*, 1. ed., Blackie Academic and Professional, London, **1998**.
- [14] N. E. Brese, M. Okeeffe, *Acta Crystallogr., Sect. B* **1991**, *47*, 192–197.
- [15] a) J. Tauc, R. Grigorov, A. Vancu, *Phys. Status Solidi* **1966**, *15*, 627–637; b) A. B. Murphy, *Sol. Energy Mater. Sol. Cells* **2007**, *91*, 1326–1337.
- [16] a) O. Merka, V. Yarovy, D. W. Bahnemann, M. Wark, *J. Phys. Chem. C* **2011**, *115*, 8014–8023; b) T. Watanabe, T. Takizawa, K. Honda, *J. Phys. Chem.* **1977**, *81*, 1845–1851; c) F. Chen, J. C. Zhao, H. Hidaka, *Int. J. Photoenergy* **2003**, *5*, 209–217.
- [17] D. Sattler, M. Schlesinger, M. Mehring, C. A. Schalley, *Chem-PlusChem* **2013**, *78*, 1005–1014.
- [18] a) K. Yu, S. Yang, H. He, C. Sun, C. Gu, Y. Ju, *J. Phys. Chem. A* **2009**, *113*, 10024–10032; b) Q. Wang, C. Chen, D. Zhao, W. Ma, J. Zhao, *Langmuir* **2008**, *24*, 7338–7345; c) H. Park, W. Choi, *J. Phys. Chem. B* **2005**, *109*, 11667–11674.
- [19] a) G. M. Sheldrick, in: *An Integrated System for Solving, Refining and Displaying Crystal Structures from Diffraction Data, Siemens Analytical X-ray Instruments*, Madison, WI, **1990**; b) G. M. Sheldrick, *Acta Crystallogr., Sect. A* **1990**, *46*, 467–473.

Received: July 12, 2013

Published Online: November 20, 2013